Trends in Environmental Analytical Chemistry 2 (2014) 1–10

Contents lists available at ScienceDirect

Trends in Environmental Analytical Chemistry

journal homepage: www.elsevier.com/locate/teac

Review

Trends and advances in mercury stable isotopes as a geochemical tracer

Runsheng Yin [a,b], Xinbin Feng [c,*], Xiangdong Li [b], Ben Yu [c], Buyun Du [c]

[a] State Key Laboratory of Ore Deposit Geochemistry, Institute of Geochemistry, Chinese Academy of Sciences, Guiyang 550002, China
[b] Department of Civil and Environmental Engineering, The Hong Kong Polytechnic University, Hung Hom, Kowloon, Hong Kong
[c] State Key Laboratory of Environmental Geochemistry, Institute of Geochemistry, Chinese Academy of Sciences, Guiyang 550002, China

ARTICLE INFO

Article history:
Received 11 February 2014
Received in revised form 17 March 2014
Accepted 18 March 2014

Keywords:
Mercury
Isotope
Mass dependent fractionation
Mass-independent fractionation
Geochemical tracer

ABSTRACT

Mercury (Hg) stable isotope geochemistry is a rapid emerging research field. During the past decade, mercury isotope geochemistry has become an essential part of mercury science, and has played an important role for a wide variety of scientific progresses relating to this metal. Recent studies have demonstrated that Hg isotopes can be systematically fractionated during specific environmental processes (*e.g.*, biotic, abiotic and photochemical). Mercury can have both mass-dependent fractionation (MDF) and mass-independent fractionation (MIF). Each fractionation process imparts a diagnostic pattern of isotopic variations on the earth's geochemical reservoirs, and thus Hg isotope ratios can be used to unravel the sources and complex biogeochemical pathways for Hg. Large variations (~10‰) of both MDF and MIF signatures have been detected in different environmental compartments. The observation of MIF in natural samples suggests that photochemical reaction of Hg species plays an important role in the global cycle of Hg. This paper reviews the analytical methods, the contrasting isotope fractionation during Hg geochemical transformation, the isotopic signatures of different geochemical reservoirs, and the potential uses of Hg isotopes in the future.

Contents

* Corresponding author. Tel.: +86 851 5891356; fax: +86 851 5891609.
E-mail address: fengxinbin@vip.skleg.cn (X. Feng).

http://dx.doi.org/10.1016/j.teac.2014.03.001
2214-1588/

1. Introduction

Mercury is a globally distributed and toxic trace metal [1–4]. The geochemical cycling of Hg (Fig. 1) involves direct emissions, atmospheric transport, deposition to land and ocean, and re-volatilization [3]. The atmosphere plays a cardinal role in the global dispersion and deposition of mercury [4]. Mercury is released to the atmosphere through natural, anthropogenic and secondary emissions [5] in the form of gaseous elemental Hg (Hg^0_g), gaseous oxidized Hg (Hg^{II}_g) and particulate/aerosol bound Hg (PHg_g). Hg^0_g is the most abundant (>95%) atmospheric Hg form with an extensive life-time of ~1 yr [1,2]. Hg^0_g is subjected to atmospheric long-range transport, and is subsequently the predominant source of Hg in pristine remote areas [6,7]. Hg^0_g is oxidized to Hg^{II}_g by ozone and reactive halogen species [8]. Hg^{II}_g and to a lesser extent Hg^0, can be associated with aerosols and particulate matter in the form of PHg_g, which is effectively removed from the atmosphere through wet and dry deposition [9]. Oceanic Hg emissions contribute to the long-range transport of atmospheric Hg through a "multi-hop" mechanism as atmospheric Hg is deposited to the ocean and then reemitted to the atmosphere [10]. Once deposited into aquatic environments, Hg undergoes complicated transformation both by biological and non-biological processes [11]. Mercury exists in the ocean mainly in inorganic forms, *e.g.*, dissolved divalent Hg (Hg^{II}_{aq}), particulate Hg (PHg_{aq}) and dissolved gaseous elemental Hg (Hg^0_{aq}) [2]. Reduction of Hg^{II}_{aq} to Hg^0_{aq} in natural waters may proceed thermally or induced by actinic radiation in the presence of suitable ligands [12]. Oceanic waters generally exhibit significant degrees of supersaturation with respect to Hg^0_{aq} [13]. The subsequent loss of Hg^0_{aq} is thought to be rapid and extends the atmospheric lifetime of Hg [14]. Conversely, Hg can exit the water through conversion of Hg^{II}_{aq} to PHg_{aq} followed by gravitational settling. The ultimate sink of PHg_{aq} is burial into the deep-ocean sediments, which occurs very slowly [11]. Bioavailable Hg^{II}_{aq} may also convert to methylmercury (MeHg), a toxin that can be effectively bio-accumulated through aquatic food webs, eventually posing a serious threat to humans and wild life [1]. Humans have altered the biogeochemical cycle of Hg by a factor of ~3. As a consequence of past and present intensive human activities and given the sluggish transfer time of ~3000 yr to sediments, an increased amount of Hg is circulating in the land-ocean-atmosphere system [3].

Research into Hg stable isotope biogeochemistry is offering new insight into the behavior of Hg [15–19]. Recent experimental work demonstrated fractionation of Hg isotopes during various processes (*i.e.*, biological [20–23] and non-biological physiochemical [24–36] processes) known to be a part of the global and regional Hg biogeochemical cycles. Large variations of both mass-dependent (MDF, represent as $\delta^{202}Hg$) and mass-independent fractionation (MIF, represent as $\Delta^{199}Hg$) (range of ~10‰ for both) are found among different source materials on the earth [15–19]. Variations in the natural abundance of Hg isotopes have shed lights on many long-standing problems in Hg science including: (1) label of Hg isotope fractionation factors to discriminate important biotic and abiotic reactions [20–36]; (2) tracing potential sources of Hg in the environment compartments [37–57]; and (3) determination of environmental materials to reveal specific geochemical processes of Hg [58–72] (Fig. 2).

Since the first precise measurement of Hg isotopes in natural samples in 2000 [73], to the Special Issue titled with "Advances in

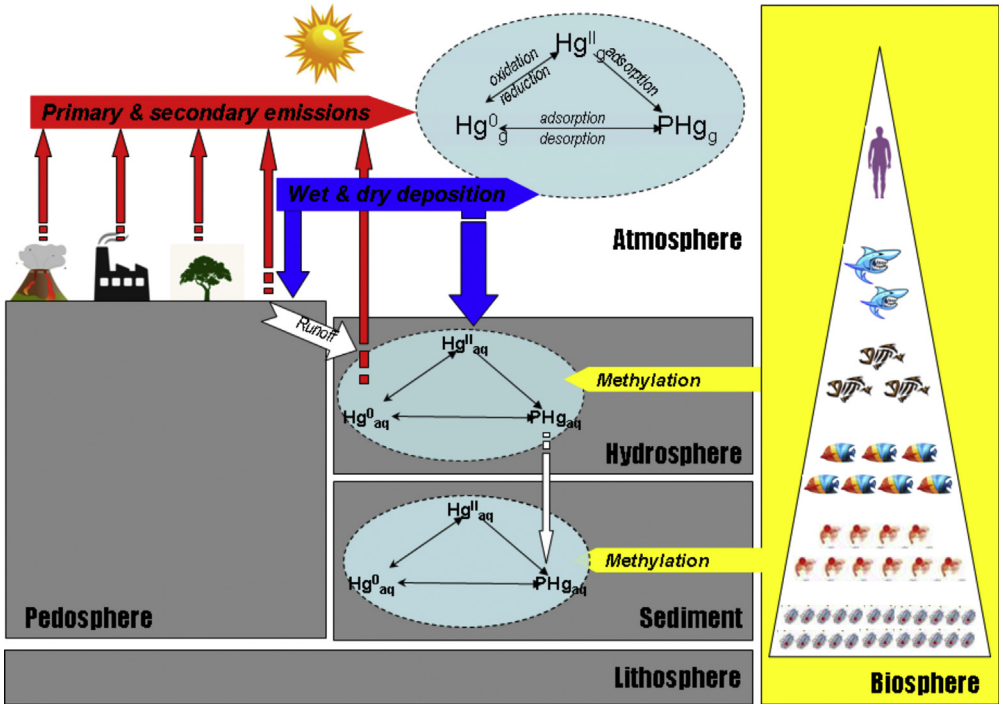

Fig. 1. Conceptual view of the global Hg biogeochemical cycle.

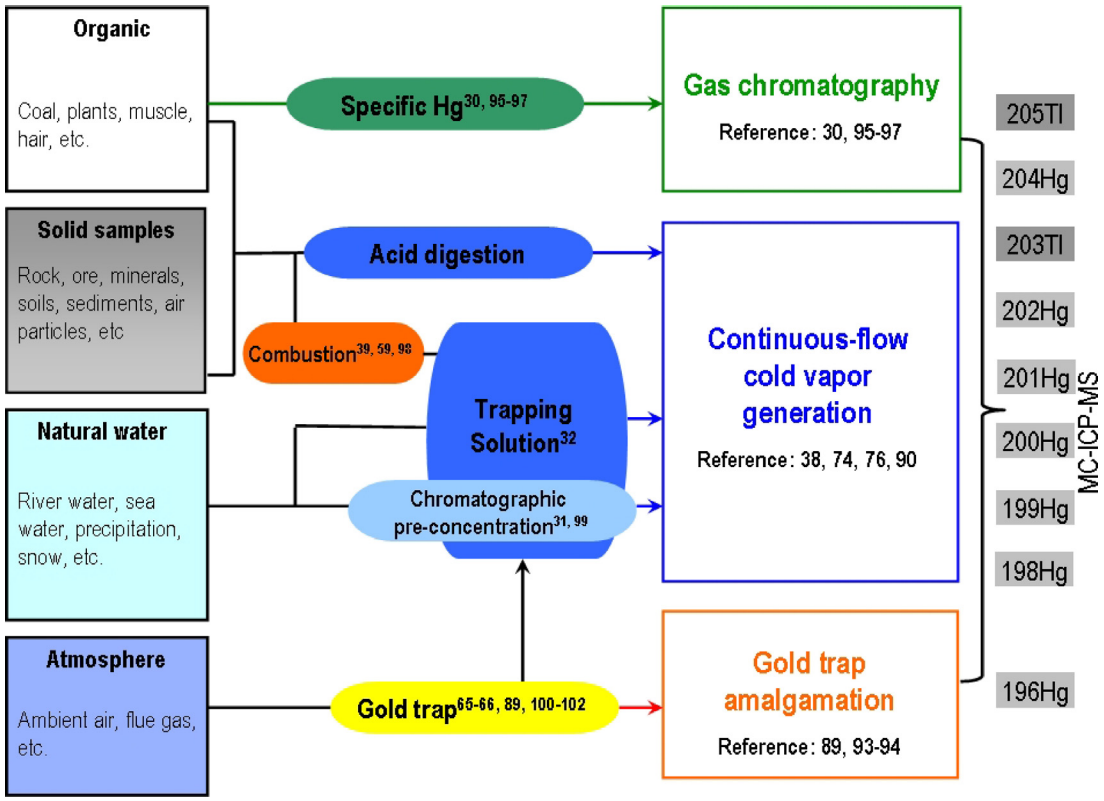

Fig. 2. Conventional diagram for measuring Hg isotope composition of different environmental samples.

Mercury Stable Isotope Biogeochemistry" published in *Chemical Geology* in 2013 [74], Hg stable isotope geochemistry has become a frontier subject in earth and environmental sciences. With more researchers becoming interested in Hg isotope geochemistry, it is critical to have a comprehensive review of the current research state of this important research field.

2. Mercury isotope analytical method

2.1. Nomenclature of mercury isotopes

Mercury has seven natural stable isotopes: ^{196}Hg (0.15%), ^{198}Hg (9.97%), ^{199}Hg (16.87%), ^{200}Hg (23.10%), ^{201}Hg (13.18%), ^{202}Hg (29.86%), and ^{204}Hg (6.87%) [75]. Two alternatives in reporting Hg isotopic differences are the absolute ratios and the deviations from a common standard [19]. Reporting the absolute ratios is challenging due to the experimental mass bias. Like other stable isotope systems, Hg isotopic variations are commonly reported as delta notations, which mean the per mil deviations from an international standard [75]:

$$\delta^{xxx}\mathrm{Hg}(‰) = \{(^{xxx}\mathrm{Hg}/^{yyy}\mathrm{Hg}_{sample})/(^{xxx}\mathrm{Hg}/^{yyy}\mathrm{Hg}_{standard}) - 1\} \times 1000 \quad (1)$$

where xxx is mass of each Hg isotope between 196 and 204 amu. The NIST SRM 3133 (10.00 ± 0.02 mg/g Hg in 10% HNO_3) solution is recommended as the universally adopted reference standard [75]. By far, ^{196}Hg is usually not measured due to its lowest abundance (0.15%). Most studies adopt ^{202}Hg/^{198}Hg (^{202}Hg has the largest abundance and ^{202}Hg and ^{198}Hg generates a relatively high fractionation compared to other isotope pairs), being consistent with other isotope systems which are expressed as heavier isotopes divided by lighter ones (*e.g.* ^{13}C/^{12}C) [75]. However, ongoing debate remains about whether the denominator should be ^{202}Hg, which is the most abundant Hg isotopes and therefore gives the highest precision in Hg isotope analysis [55,56].

MIF of Hg isotopes is reported using Δ^{xxx}Hg, which means the deviation of the measured isotope ratio from the theoretical ratio predicted by MDF:

$$\Delta^{xxx}\mathrm{Hg} \approx \delta^{xxx}\mathrm{Hg} - (\delta^{202}\mathrm{Hg} * \beta) \quad (2)$$

where β is the scale factor of the theoretical MDF law for kinetic and equilibrium fractionation, respectively [76].

$$\beta_{\mathrm{kinetic}} = \frac{\ln(m_{198}/m_x)}{\ln(m_{198}/m_{202})} \quad (3)$$

$$\beta_{\mathrm{equilibrium}} = \frac{(1/m_{198} - 1/m_x)}{(1/m_{198} - 1/m_{202})} \quad (4)$$

To describe the isotopic fractionation between the reactants and products during geochemical processes, the fractionation factor (α^x_{A-B}) was used:

$$\alpha^X_{A-B} = \frac{(^{xxx}\mathrm{Hg}/^{yyy}\mathrm{Hg})_A}{(^{xxx}\mathrm{Hg}/^{yyy}\mathrm{Hg})_B} \quad (5)$$

Since α is usually close to unity, it is commonly to use the ε^x_{A-B} notation when describing differences in isotopic composition [77]. The ε^x_{A-B} notation has the advantage over using 1000 lnα of being a more exact expression of the per mil fractionation:

$$\varepsilon^X_{A-B} = 1000(\alpha^X_{A-B} - 1) \approx 1000\ln a \quad (6)$$

2.2. Development of mercury isotope analytical techniques

The measuring of Hg isotopes has a remarkably long history. In 1919, Aston [78] discovered the existence of natural stable Hg

isotopes. Soon after that, Brønsted and von Hevesy [79] managed to separate the Hg isotopes during evaporation-condensation process using high precision density measurements. In 1950, Nier [80] reported Hg isotopic variations in natural samples based on the gas-source mass spectrometry measurements. However, their data were later called into questions due to its large analytical uncertainty (<±20‰) [81]. Hg isotopic measurements of meteorolite samples were followed after neutron activation analysis (NAA), which was also viewed with some skepticism [82].

Instrumental improvement in inductively coupled plasma mass spectrometry (ICP-MS), *e.g.*, inductively coupled plasma time-of-flight mass spectrometry (ICP-TOF-MS) [83], quadrupole (Q-ICP-MS) [84] and single collector magnetic sector ICP-MS [85] have greatly improved the precision of isotopic measurements. However, each of these techniques exhibits certain disadvantages for high precision Hg isotope measurements. ICP-TOF-MS offered simultaneous detection of multiple isotopes but it suffers from low sensitivity. Other ICP-MS only have a single detector are able to the measure the multiple isotopes sequentially in time [19]. Finally, a multi-detector arrangement is required. Thermal ionization mass spectrometry (TIMS) with multi-detectors is widely used to perform very precise isotopic measurements for elements with low ionization potentials. However, the high ionization potential of Hg makes TIMS unable to measure [86]. The multiple-collector inductively coupled plasma mass spectrometry (MC-ICP-MS) combines the multi-detectors with very high ionization efficiency of the ICP source, allowing very high precision isotopic analysis for various elements with high ionization potentials (*e.g.*, Hg) that was previously impracticable to analyze [37]. Today, Hg isotope compositions are measured exclusively using MC-ICP-MS, and the precision of which is at least one order of magnitude better than other techniques [19].

2.3. Mass bias correction

High precision analyses of Hg isotopes require proper mass bias corrections. Minimization of the methodological mass bias needs to keep the methods and conditions of sample preparation and analysis as constant as possible. For a series of samples whose isotope abundances are to be compared with each other (*e.g.*, a sequence of core sections), they should be analyzed in a single continuous run under uniform conditions. Another crucial topic is the interference of other elements (*e.g.*, ^{204}Pb interferes with ^{204}Hg) [60]. Hence, confirmation tests are needed to check for interference. For instance, Jackson et al. [60] used ^{206}Pb and ^{195}Pt measurements to correct for interference between ^{204}Pb and ^{204}Hg, and between ^{196}Pt and ^{196}Hg, respectively.

Accurate instrumental mass bias corrections are of great importance for MC-ICP-MS analysis. Three optional instrumental mass bias correction categories are recommended [75], including: (a) external correction by measuring the isotope ratio of another element, *e.g.*, Tl [37,75,87–89]; (b) bracketing the sample with a standard (*e.g.*, NIST SRM 3133) of known isotope composition; and (c) isotope double-spike method, where two additional Hg isotopes with a known ratio were added to the samples [90]. Most available methods adopted a combination of strategies (a) and (b), and gained a high precision Hg isotope analysis [37,75,87–89]. Perhaps, the standard-sample-standard bracketing method is the only essential method for Hg isotope determination. There is the concern that the Tl isotopes themselves may be subject to mass bias effects, thereby adding to the analytical uncertainty. Mead and Johnson [90] performed the double-spike internal mass-bias correction using ^{196}Hg and ^{204}Hg, and achieved similar precisions with the more widely standard-sample-standard bracketing protocol.

2.4. Analytical uncertainty

Knowing the analytical uncertainty of each measurement is important in evaluating the Hg isotopic data. The first key issue is to know the internal precision of an isotopic measurement. Internal precision is usually calculated as the standard error (SE) obtained from measurements of the same sample accumulated during a single analytical run. This value is an indication for the precision of the individual measurement [17,19]. Another important issue is the reporting of the external precision, which is defined as the standard deviation (SD) observed for replicate analysis of a sample. The external precision is commonly considered as the reproducibility of the overall method. This can be assessed by preparing the replicate ($n \geq 3$) samples [19]. For samples with amount insufficient to do replicate Hg isotope analysis, a reference standard material with matrix close to the sample should be measured repeatedly to give the external reproducibility. Finally, to ensure the accuracy of each measurement and evaluate the data obtained in different laboratories, a secondary standard with distinct isotopic composition from the bracketing standard should be measured. Measured isotopic composition for the secondary standard should be consistent for each analytical session. UM-Almadén was recommended as an inter-laboratory comparison standard [75]. However, one problem of the UM-Almadén is that it is only ~0.5‰ different to the primary standard (NIST SRM 3133). Thus, large MDF ranges are poorly calibrated with only UM-Almadén. Estrade et al. [91] provided two additional secondary Hg isotope reference materials with a large range of MDF for distribution in the Hg research community.

2.5. Different ways to introduce mercury into the MC-ICP-MS

2.5.1. Gold trap amalgamation (GTA)

The GTA technique, which is commonly used for quantitative Hg determination, has been chosen for many Hg isotopic measurements [92,93]. The GTA technique makes the potential to measure Hg isotopic composition with very low Hg levels (*e.g.*, atmosphere Hg) [19]. The GTA drastically enhances the detection sensitivity though its effectiveness in Hg pre-concentration. However, when heating up a gold trap, it usually produces a transient signal. As MC-ICP-MS are optimized based on steady signals which vary only little in intensity, large internal precision during the peak evolution was observed [92]. Subsequent modifications aimed to extending and flattening the peak can improve the precision and accuracy of the method, and succeed in improving the internal precisions [93].

2.5.2. Continuous-flow cold vapor generation (CCVG)

The demand in generating the steady signal during Hg isotope analysis has used the CCVG as the choice for sample introduction [37,73,75,89]. Practically, the sample solution (before using the CCVG, it is necessary to convert all the Hg in samples to dissolved Hg^{II} species using oxidizing acids) is continuously mixed with a reducing solution (*e.g.*, stannous chloride) using peristaltic pumps and argon gas is introduced into a gas-liquid separator. The gaseous Hg vapor is stripped from solution and transported to the MC-ICP-MS, while the waste solution is discarded in order to obviate any possible matrix effects [37,73,75,89]. Under optimal analytical conditions and including complete separation of Hg from the sample matrix, the analysis of matrix-matched bracketing standards of the same concentration can be performed with careful monitoring of background signals, and on-peak blank corrections.

The analytical precision of ±0.10‰ (2 SD) for δ^{202}Hg and ±0.05‰ (2 SD) for Δ^{199}Hg can be achieved [75].

2.5.3. Gas chromatography (GC)

The GC enables simultaneous measurement of the isotope ratios of specific Hg compounds, such as MeHg [29,94–96]. Similar to the GTA method, this GC also generates transient signals, which caused difficulties in precise measurements of isotope ratios. Another disadvantage for the GC is that isotope ratios may change during Hg elution process from the GC column. Further improvements should be carried out to solve this problem.

2.6. Pretreatment of sample with different matrices

Among various sample introduction strategies, the CCVG is widely applied for Hg isotope analysis [37,73,75,89]. The CCVG requires adjusting the total Hg concentrations in the sample and standard solutions to 1–5 ng/mL of concentrations [37,73,75,89] which is optimal because the concentrations in that range (1) are high enough to ensure an acceptable level of precision, and yet (2) are low enough to minimize the flushing time needed to eliminate possible "memory effects" due to insufficient flushing between consecutive analyses. Hence, operational pre-treatment protocols are needed for samples with different Hg levels.

- **Solid samples** can be fully digested using oxidizing acids, and diluted after Hg is fully oxidized. The use of acid during digestion may increase the risk of Hg contamination. An alternative choice is that Hg in samples can be thermal-released and trapped using either GTA or oxidizing solutions (*e.g.*, $H_2SO_4 + KMnO_4$, or $HNO_3 + HCl$) [38,58,97], and then analyzed by MC-ICP-MS. Such protocol is particularly useful for solid samples with low Hg contents (*e.g.*, peat, coal, pristine soil/sediment).
- **Water samples**. Hg in waters can be reduced using $SnCl_2$, and the produced Hg^0 can be trapped by trapping solution [17]. Another possible matrix separation method would be column chemistry [30,98]. Chen et al. [98] developed a new pre-concentration technique using AG 1 × 4 ion-exchange resin. This technique resulted in acceptable procedural blanks and quantitative yields (101% ± 6%) in the final Hg eluates, and thus validated the measurement of Hg isotope composition in low Hg water samples [98].
- **Atmospheric samples**. Few studies have investigated the mercury isotopic composition in different atmospheric Hg species, *e.g.*, Hg^0_g, Hg^{II}_g, and PHg_g [64,65,88,99–101]. In general, Hg^0_g was collected used oxidizing solution [71] and/or GTA [64,65,88,99–101]; PHg_g was collected using quartz fiber membrane [100,101]; and Hg^{II}_g was collected by quartz fiber filters treated with potassium chloride [101]. Measuring isotopic compositions of atmospheric Hg is challenging due to the fact that the Hg concentration is low. This is especially true for Hg^{II}_g and PHg_g, which are typically present in the atmosphere at $<10\ pg/m^3$ levels in uncontaminated rural environments [1–4,101].

3. Theory in isotope fractionation of mercury

Hg has seven stable isotopes (196–204 amu) with a mass difference of 4%, active redox chemistry, a volatile form, and a tendency to form covalent bonds, thus providing many opportunities for isotopic fractionation. The ability of using stable isotope ratios of Hg as an indicator of Hg biogeochemical processes in environmental studies depends on well-founded constraints on the extent of fractionation (*i.e.*, values of fractionation factors) during all the transformation processes known to be a part of the global and regional Hg biogeochemical cycles [18,20–36,77]. Recent experimental work demonstrated the fractionation of Hg isotopes during various geochemical processes, including micro-mediated reactions (*e.g.*, reduction [20,21], methylation [22] and de-methylation [23]), non-biotic chemical reactions (*e.g.*, photo-reduction [24–26], chemical reduction [27,28], methylation [29] and de-methylation [24,30]), and physical processes (*e.g.*, volatilization [31], evaporation [32], adsorption [33,34], leaching [35] and diffusion [36]). Each fractionation process imparts a diagnostic pattern of isotopic variation, and thus Hg isotope ratios can be used to unravel the sources and complex biogeochemical pathways of Hg. Table 1 summarizes the experimental studies conducted to date, which detected and quantified ε_{A-B} during distinct

Table 1
Direction and magnitude of mercury isotope fractionation during different biogeochemical processes.

Geochemical processes	Type of process	Reactant (B)	Product (A)	Experimental conditions	MDF ε_{A-B}(‰)	Type of MIF	References
Abiotic chemical reactions							
Photo-reduction of Hg^{II}_{aq}	Kinetic	Hg^{II}	Hg^0	Fulvic acid	−0.60	MIE	[24]
Photo-reduction of Hg^{II}_{aq}	Kinetic	Hg^{II}	Hg^0	Formic acid	−1.34	NVE	[27]
Photo-reduction of Hg^{II}_{aq}	Kinetic	Hg^{II}	Hg^0	Bulk DOM	−1.06	MIE	[25]
Photo-reduction of Hg^{II}_{aq}	Kinetic	Hg^{II}	Hg^0	Cysteine	−1.32	MIE	[26]
Photo-reduction of Hg^{II}_{aq}	Kinetic	Hg^{II}	Hg^0	Serine	−1.71	MIE	[26]
Photo-demethylation	Kinetic	MeHg	Hg^0	Fulvic acid	−1.30 to −1.70	MIE	[24]
Photo-demethylation	Kinetic	MeHg	Hg^0	Vary with pH, and radical scavengers	−0.13 to −0.36	MIE	[30]
Non photo-reduction of Hg^{II}_{aq}	Kinetic	Hg^{II}	Hg^0	Dark organically medicated reduction	−1.70	MIE	[24]
Non photo-reduction of Hg^{II}_{aq}	Kinetic	Hg^{II}	Hg^0	Bulk DOM	−1.52	NVE	[28]
Non photo-reduction of Hg^{II}_{aq}	Kinetic	Hg^{II}	Hg^0	$SnCl_2$	−1.56	NVE	[28]
Abiotic ethylation	Kinetic	Hg^{II}	Hg^0	$SnCl_2$ and $NaBH_4$	−1.17	NVE	[27]
Abiotic ethylation	Kinetic	Hg^{II}	Hg^0	Abiotic, $NaBEt_4$ as ethylation reagent	−1.08	MDF	[27]
Hg^0_{aq} volatilization	Kinetic	Hg^0_{aq}	Hg^0	Dissolved Hg^0 in water solution to Hg^0	−0.47	MDF	[31]
Elemental Hg evaporation	Kinetic	Hg^0	Hg^0	Vacuum evaporation of elemental Hg^0	−6.68	NVE	[32]
Abiotic methylation	Kinetic	Hg^{II}	MeHg	Methylcobalamin in aqueous chloride	−0.70	MDF	[29]
Elemental Hg evaporation	Equilibrium	Hg^0	Hg^0	Equilibrium between metallic Hg and Hg^0 vapor	−0.86	NVE	[32]
Hg–thiol complexation	Equilibrium	Hg^{II}	Hg^{2+} thiol	Hg^{2+} to Hg^{2+}–thiol	−0.53 to −0.62	NVE	[33]
Biotic chemical reactions							
Microbial reduction of Hg^{II}_{aq}	Kinetic	Hg^{II}	Hg^0	*Escherichia coli JM109/Ppb117*	−1.4 to −2.0	MDF	[20]
Microbial reduction of Hg^{II}_{aq}	Kinetic	Hg^{II}	Hg^0	*Bacillus cereus Strain 5*	−1.2 to −1.4	MDF	[21]
				Anoxybacillius sp Strain FB9			
Microbial reduction of Hg^{II}_{aq}	Kinetic	Hg^{II}	Hg^0	*Shewanella oneidensis MR-1*	−1.80	MDF	[21]
Microbial methylation	Kinetic	Hg^{II}	MeHg	*Desulfobulbus propionicus*	−2.60	MDF	[22]
Microbial de-methylation	Kinetic	MeHg	Hg^0	*Escherichia coli JM109/pPB117*	−0.40	MDF	[23]

biogeochemical transformations [20–36]. Like stable isotope fractionation of light elements (*e.g.*, H, C) [102], most processes (both kinetic and equilibrium) fractionate Hg isotopes according to their masses, with light Hg isotopes preferentially reacted and enriched in the products ($\varepsilon_{A-B} < 0$) [20–33].

MIF refers to any geochemical process that fractionates isotopes, where the amount of separation does not scale in proportion with the difference in the masses of the isotopes. MIF effects had already been documented for O, S, and a number of metallic elements (*e.g.*, Ti, U, Zn, Cd, and Pb) [103,104]. The MIF signature of odd Hg isotopes was firstly reported in aquatic organisms [24,59,60] and was later observed by several laboratory experiments (Table 1). The MIF of odd Hg isotopes is generally understood by nuclear volume effect (NVE) [105,106] and magnetic isotope effect (MIE) [107,108]. The NVE originates from the effect of nuclear volume on electrons. Variations in nuclear size and shape change the nuclear charge distribution, which results in a slightly different electrostatic field to interact with electrons having a high density at the nucleus (*i.e.*, s orbital electrons) [105,106]. The MIE is a kinetic fractionation that appears to occur primarily during photochemical radical pair reactions [107,108]. Laboratory experiments observed NVE during several processes, *e.g.*, elemental Hg volatilization [32], non-photo reduction of Hg species [25,28], and Hg-thiol complexation [33]. Elemental Hg volatilization experiments demonstrated $\Delta^{199}Hg/\Delta^{201}Hg$ of 2.0 [32], non-photo reduction of Hg^{2+} produced $\Delta^{199}Hg/\Delta^{201}Hg$ from 1.5 to 1.61 [25,28], and equilibrium Hg-thiol complexation induce $\Delta^{199}Hg/\Delta^{201}Hg$ of 1.54 [33]. As shown in Fig. 3, the MIE showed a different pattern of $\Delta^{199}Hg/\Delta^{201}$ from the NVE. The MIE has been proven during the photo-reactions of aqueous Hg in the presence of dissolved organic carbon (DOC) [24–26]. Photo-reduction of Hg^{II}_{aq} and photo degradation of MeHg produces $\Delta^{199}Hg/\Delta^{201}Hg$ ratios of 1.0 and 1.36, respectively [24]. Recent evidence demonstrated that biochemical mediated processes also cause MIE. Buchachenko et al. [109] postulated that thiyl radicals, which are commonly generated by various biochemical reactions, may also cause MIE.

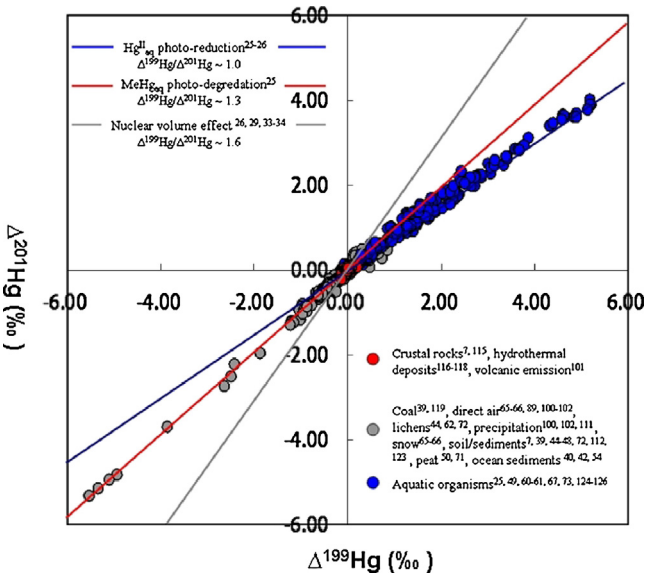

Fig. 3. $\Delta^{199}Hg/\Delta^{201}Hg$ of mass independent fractionation of Hg isotopes.

Jackson et al. [55–57,59,60] presented evidence that MIF can be caused by microbial activities in aquatic ecosystems.

Large variation of MIF ($\Delta^{199}Hg$: ~10‰) has been observed in the environmental compartments (Figs. 3 and 4). Among various processes, photo-chemical reactions may be of global importance to the observed MIF as they generate the highest Hg MIF. Other processes (*e.g.*, non-photochemical reactions, evaporation, and Hg-thiol complexation) produce Hg MIF in almost one order of magnitude lower (<0.2‰ for $\Delta^{199}Hg$) [25,28,32,33]. As detailed in Section 4, the observations of continental compartments (*e.g.*, soils, lichens, plants) that mainly received Hg from atmospheric deposition have shown predominantly negative MIF, while aquatic environment compartments (*e.g.*, fishes, waters and ocean

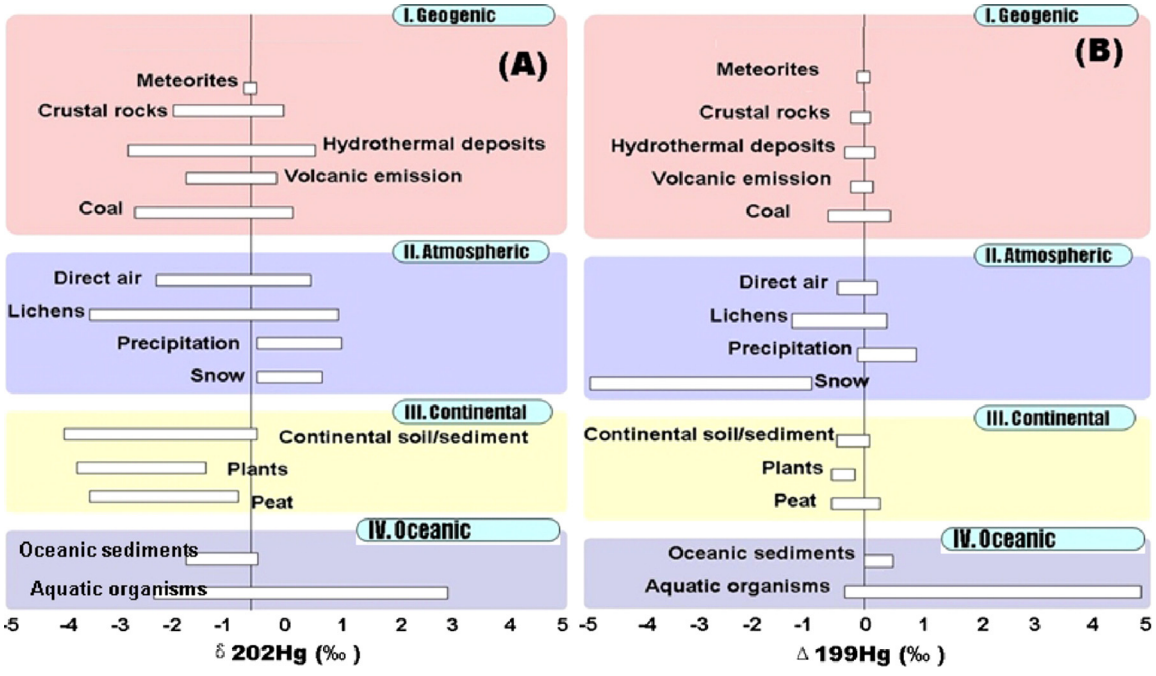

Fig. 4. Summary of published data (A: $\delta^{202}Hg$ values; B: $\Delta^{199}Hg$ values) of earth samples. Data sources: Meteorites[82], crustal rocks[7,113], hydrothermal deposits[114–116], volcanic emission[100], coal[38,117], direct air[64,65,88,99–101], lichens[43,61,71], precipitation[99,101,110], snow[64,65], continental soil/sediments[7,38,43–47,71,111,121], peat[49,70], ocean sediments[39,41,53], aquatic organisms[24,48,59,60,66,72,122–124].

sediments) have shown adverse positive MIF. This has led to the speculation that photo-induced reactions of aquatic Hg (*e.g.*, Hg^{II}_{aq} and MeHg) is the plausible inducing reactions to the global MIF, as photo-reactions of aqueous Hg resulted in releasing Hg^0 with negative MIF, leaving the remaining Hg with positive MIF signatures [24–26]. As shown in Fig. 3, natural samples mainly containing Hg^{II} showed $\Delta^{199}Hg/\Delta^{201}Hg$ of ~1.0, and samples predominant containing MeHg showed $\Delta^{199}Hg/\Delta^{201}Hg$ of ~1.3, which is in accordance with the $\Delta^{199}Hg/\Delta^{201}Hg$ produced by photo-reduction of Hg^{II}_{aq} and photo degradation of MeHg, respectively [18].

A few recent studies demonstrated MIF of even Hg isotopes (^{200}Hg and ^{204}Hg) in precipitations and atmospheric Hg species [99,101,110,111]. MIF of even Hg isotopes has been linked to Hg^0_g photo-oxidation occurring on the particle and aerosol surfaces [99,110]. Mead et al. [90] observed larger MIF of both even and odd Hg isotopes in an unknown pattern in fluorescence light bulbs, which may be partially explained by photochemical self-shielding. MIF of even Hg isotopes has not been tested or verified by any experiments [110,111,90]; further studies using proper normalization ratios can help to figure out whether it is really ^{200}Hg which exhibits an anomaly or whether all Hg isotopes have been fractionated by an unknown MIF process.

4. Field observations of mercury isotopes

Studies up to date have established the isotope signatures of major geochemical reservoirs in the earth system, ranging from the Earth's crust, surface, hydrosphere to atmosphere (Fig. 4). The MDF and MIF recorded in natural environmental samples can contribute to the understanding and quantification of sources and important processes in the global cycle of Hg. With the increasing data of natural variations in Hg isotope composition, a critical issue for geochemist is to understand how they are related to the biogeochemical cycling of Hg.

4.1. Natural and anthropogenic sources

Mercury emitted to the environment can be categorized as natural (*e.g.*, volcanic and hydrothermal emissions), anthropogenic (*e.g.*, metallurgical mining, coal combustion) and secondary sources [3,5]. Both natural and anthropogenic sources transfer Hg from long-lived lithospheric reservoirs to the atmosphere. Primary anthropogenic sources release 1900–2900 Mg/yr compared with primary natural inputs of 80–600 Mg/yr [112]. Most lithospheric samples show relatively narrow range of MDF ($\delta^{202}Hg$: ~ −0.70‰) and insignificant MIF ($\Delta^{199}Hg$: ~0‰) [58,113]. For instance, hydrothermal fluids from the crustal rocks has a mean $\delta^{202}Hg$ of -0.86 ± 0.97‰ (1SD, $n = 32$) [63]. Volcanic emission showed a similar isotope signature to the crustal rocks and the hydrothermal fluids [100]. Primary anthropogenic Hg emissions have increased the amount of lithospheric Hg to the environment. Metallurgical mining originates from refining of hydrothermal minerals, *e.g.*, cinnabar, sphalerite [3,5,114]. Published data of hydrothermal minerals fall well within the range of crustal systems [115–117] (Fig. 4). The isotopic composition of Hg in coals was investigated by several studies [38,97,118–120]. Mercury in coal showed a different pattern from that of other sources (Fig. 4) [38,97,118–120]. Coal received mercury from syngenetic (depositional) and epigenetic (hydrothermal) Hg sources [118]. Distinct isotopic signature of Hg has been observed in syngenetic and epigenetic sources of Hg in coals in Illinois Basin, USA. [118]. Studies of coal samples revealed significant MIF of approximately 1‰ in $\Delta^{199}Hg$ values with $\Delta^{199}Hg/\Delta^{201}Hg$ of ~1, suggesting certain Hg sources has been undergone photo-reduction prior to incorporation in coals [118–120].

Primary natural and anthropogenic source of Hg deposited to lands and oceans can reduce to Hg^0 and re-emit as secondary Hg sources [112]. Many processes are able to fractionate Hg isotopes during secondary Hg emission processes. Photo-reduction [24–27], volatilization [30,31], microbial reduction [20,21] induce kinetic MDF of Hg isotopes, producing elemental Hg with lower $\delta^{202}Hg$ values than that of the residual Hg pool. The ocean plays a critical role in the global cycling of Hg. Field and laboratory studies have suggested that photolytic processes drive most Hg^{II}_{aq} reduction in ocean surface waters. Aqueous photo-reduction of Hg species results in releasing of Hg^0 with negative MIF that is subsequently taken up and redistributed within and among ecosystems [112].

4.2. Atmospheric mercury

Direct analyses of Hg isotopic composition in different atmospheric Hg species were conducted by a number of studies [64,71,88,99–101,111]. Hg^0_g comprises >95% of Hg in the atmosphere [1,2]. Hg^0_g showed large variations of both $\delta^{202}Hg$ and $\Delta^{199}Hg$ values among different regions. For instance, Zambardi et al. [100] collected Hg^0_g ($\delta^{202}Hg$: −1.74‰; $\Delta^{199}Hg$: ~0) in a fumarole plume from an active volcano in Italy; Gratz et al. [99] measured Hg^0_g ($\delta^{202}Hg$: −0.59‰ to +0.43‰; $\Delta^{199}Hg$: −0.21‰ to +0.06‰) in the Great Lakes, USA. Sherman et al. [64] investigated ambient Hg^0_g ($\delta^{202}Hg$: −0.12‰ to +0.15‰; $\Delta^{199}Hg$: −0.11 to −0.22‰) near Barrow, Alaska; Rolison et al. [101] investigated the isotopic composition of Hg^0_g ($\delta^{202}Hg$: −3.88‰ to −0.33‰; $\Delta^{199}Hg$: −0.41‰ to −0.03‰) in the Grand Bay, USA; Yin et al. [71] reported the ambient air ($\delta^{202}Hg$: −2.32‰ to −1.85‰; $\Delta^{199}Hg$: −0.34‰ to −0.24‰) in rice paddies in Wanshan Mercury Mine, China; Demers et al. [111] demonstrated the total atmospheric Hg ($\delta^{202}Hg$: +0.48‰ to +0.93‰; $\Delta^{199}Hg$: −0.21‰ to −0.15‰) in forest in Rhinelander, NE Wisconsin, USA. Such regional differences could be explained by the complicated atmospheric sources, *e.g.*, evaporation of Hg^0_g from the soil and vegetation, local anthropogenic emissions, and long-range transport of Hg^0_g. It should be noted that all above studies, except Gratz et al. [99], reported negative $\Delta^{199}Hg$ values in the Hg^0_g pool [101,110,111], which is expected to be associated with photo-reduction of Hg^{II}_{aq} [15,25]. Epiphytic lichens, which uptake Hg from ambient air, also showed negative MIF signatures [43,61,71].

Hg^0_g is oxidized to Hg^{II}_g by ozone and reactive halogen species [8]. Hg^{II}_g associated with PHg_g can be effectively removed from the atmosphere through wet/dry deposition [8,9]. Much heavier $\delta^{202}Hg$ values and positive MIF in Hg^{II}_g ($\delta^{202}Hg$: +0.51‰ to +1.61‰; $\Delta^{199}Hg$: −0.28‰ to +0.18‰) and PHg_g ($\delta^{202}Hg$: −1.61‰ to −0.12‰; $\Delta^{199}Hg$: +0.36‰ to +1.36‰) species were observed in comparison with Hg^0_g ($\delta^{202}Hg$: −3.88‰ to −0.33‰; $\Delta^{199}Hg$: −0.41‰ to −0.03‰) in the Grand Bay, USA [101]. Precipitations from several sites, *e.g.*, Great Lakes (USA) ($\delta^{202}Hg$: −0.79‰ to +0.18‰; $\Delta^{199}Hg$: +0.04‰ to +0.52‰) [99], NE Wisconsin (USA) ($\delta^{202}Hg$: −0.74‰ to 0.06‰; $\Delta^{199}Hg$: +0.16‰ to +0.82‰) [111], and Peterborough (Canada) ($\delta^{202}Hg$: −0.02‰ to +1.48‰; $\Delta^{199}Hg$: 0.29‰ to +1.13‰) [110], also showed relative heavier $\delta^{202}Hg$ and positive MIF signatures. The shift of Hg isotopic signature between Hg^0_g and precipitations (mainly containing Hg^{II}_g and PHg_g) could be explained by the photo-reduction of Hg species in cloud droplets containing organic matters, as cloud droplets would preferentially retain odd isotopes thereby becoming increasingly positive with respect to $\delta^{202}Hg$ and $\Delta^{199}Hg$ values [99,101,110].

The MIF of even Hg isotopes is established as an important feature for precipitations and atmospheric Hg species. For instance, Gratz et al. [99] firstly observed the anomalies of ^{200}Hg in precipitations from the Great Lakes, USA, and Chen et al. [110] reported more obvious MIF of ^{200}Hg ($\Delta^{200}Hg$ up to +1.24‰) in precipitations from Peterborough, Canada. Significant MIF of ^{200}Hg

was observed in atmospheric Hg species in the Grand Bay (USA), with Hg^0_g showing negative Δ^{200}Hg values (−0.19‰ to −0.06‰) while Hg^{II}_g and PHg_g showing positive Δ^{200}Hg values (+0.06‰ to +0.28‰) [101]. As mentioned in Section 3, mechanisms of the MIF of even Hg isotopes are not well understood, more research are needed in the future [110,111,90].

4.3. Terrestrial ecosystems

Reservoirs that collect atmospheric Hg deposition, such as ground vegetation and soils, may pick up the atmospheric Hg isotope anomalies. Terrestrial vegetation accumulates Hg *via* absorption of wet/dry atmospheric Hg deposition and/or through incorporation of Hg^0_g by stomata of leaves [71,111]. Available studies indicated that the consumption of Hg by plant is unlikely to induce Hg MIF [71]. However, Hg could undergo MDF during plant uptake atmospheric Hg, with the lighter isotopes preferentially incorporated by foliage. For instance, Demers et al. [111] demonstrated a MDF of ~ 3.0‰ in δ^{202}Hg values between the total atmospheric Hg and the Aspen foliage in a pristine forest in NE Wisconsin, USA. Yin et al. [71] observed a shift of ~ −1.0‰ in δ^{202}Hg values between the total atmospheric Hg and the rice foliage in Wanshan Mercury Mine (China).

Large variations of Hg isotopes have been reported in soils (Fig. 4). Surface soils received Hg mainly from geological sources and atmospheric deposition. Atmospheric Hg constitutes a minor portion in soils from Hg enriched areas (*e.g.*, mercury mines), and hence they are characterized by less MIF signatures [44,71,121]. Pristine soils have a different situation with those of geological enriched areas [7,38,43–47,111]. Hg^0_g with negative MIF entering the stomata of foliage are subsequently deposited to soil as litter fall Hg inputs [7,38,111]. This input, supplemented by wet/dry Hg deposition, is immobilized by soil organic matter probably through binding by reduced sulfur functional groups [7,38,111]. Published data on atmospheric Hg and plants overlap with the Hg isotopic compositions of continental soils, suggesting pristine soils mainly received Hg from air deposition [7,38,111]. Hg supply from mining, industrial activities, or wastewater can overwhelm inputs from atmospheric deposition and natural sources in localized areas of elevated contamination [43,47].

4.4. Aquatic ecosystems

Hg released into aquatic environments can undergo complicated transformation both by biological and non-biological processes [11]. Reduction of Hg^{2+} to Hg^0 in waters may proceed thermally or induced by actinic radiation in the presence of suitable ligands [14]. Scavenging of aqueous Hg by organic-rich particles is an important sink of Hg in waters. Sedimentation of organic particles has demonstrated no significant change of the Hg isotopic composition of a given Hg input [39]. Hence, sediment has been used as an agent in many studies to investigate the temporal [41,47] and spatial [39,42,45,51,52] variations of Hg sources in the aqueous environment. Freshwater sediments are largely impacted by riverine input of continental soils, and retain negative MIF as negative MIF values have been proven in terrestrial compartments [45,47]. Marine sediment showed a converse pattern from the terrestrial sediment [39,41,53]. The positive MIF has been reported in mid-Pleistocene Mediterranean sapropel sediments (Δ^{199}Hg: +0.11 ± 0.06‰, 2ó) [41]. Positive MIF of odd Hg isotopes in the aquatic environment was also proven by direct measurements of water [98] and marine biota [24,48,59,60,66,72,122–124]. MeHg is the dominate Hg species in aquatic organisms, Hg accumulated by food web organisms in aqueous environments shows positive MIF (Δ^{199}Hg up to +5.0‰, Fig. 4) [24,48,59,60,66,72,122–124]. Aquatic organisms showed a Δ^{199}Hg/Δ^{201}Hg: ~1.30, which is consistent with the photo-degradation of MeHg in laboratory experiments, and indicated that MeHg has undergone photo-degradation prior to incorporation into the fishes [24,48,66,72,122–124]. However, Jackson et al. [59,60] proved additional evidences that MIF might be caused by microbial activities in the aquatic environment.

5. Mercury isotopes as geochemical tracers

5.1. Tracing spatial and temporal mercury contamination

Anthropogenic activities have significantly altered the temporal and spatial patterns of Hg in the environment [112]. The distinction of anthropogenic Hg is critical to understand the magnitude of human disturbances to the natural cycle. Mercury isotopes have been used as a tool to trace and quantify Hg contamination sources in the environment [39–53]. Foucher et al. [39] gave the first example on tracking Hg sources using Hg isotopes. They demonstrated a remarkable Hg isotope difference between sediments in the Hg Idrija mining region (Slovenia) and the Gulf of Trieste (Italy). They quantified the contribution of each sources using a simple binary mixing model. Based on the well defined end-members with distinct Hg isotope signatures, recent studies also demonstrated triple mixing models to quantify the relative contributions of more than two Hg sources [51–53]. However, in certain cases, source-related signatures of Hg isotopes may be subject to alteration or obliteration by natural processes when the Hg is discharged into the environment [54–57]. A particularly good example of this is provided by Jackson et al. [56], who investigated Hg isotopes in sediment cores from three lakes situated 3.8–21.0 km from a smelter which was a point source of atmospheric Hg. They found that preservation of a detectable trace of the isotope signature of the smelter was limited to the lake closest to the smelter (*i.e.* only 3.8 km away). In other lakes, the signature of the source of pollution had apparently been completely obliterated by natural processes (probably microbial activities) in the lakes. These findings raise some doubts about the usefulness of Hg isotopes as tracers, especially in an environment far away from the sources of contamination.

5.2. Tracing mercury bioaccumulation in food webs

Similar to δ^{15}N and δ^{13}C, one of the great potentials of using Hg isotopes is to understand Hg bioaccumulation in biota. To evaluate the possibility that MIF might be produced within the fish, Das et al. [123] analyzed the Hg isotopic composition in food chains at different trophic levels from a freshwater lake (Lake Jackson, Florida, USA). They found a striking correspondence between trophic level and Δ^{199}Hg and Δ^{201}Hg values among the food chains. Jackson et al. [60] also observed an increase of Δ^{199}Hg with trophic level in their food web study. Das et al. [123] explained that the *in vivo* MIF of mercury isotopes may occur during the bioaccumulation and biomagnifications of MeHg in fish, while Jackson et al. [60] argued the MIF variations among the food web was due to the bias of inorganic Hg with different MIF signatures. Buchachenko et al. [109] predicted that thiyl radicals, being commonly involved by various biological processes, can cause the MIF in biological samples. Jackson et al. [59,60] also demonstrated the MIF occurred in the external environment was caused by microbial Hg methylation or demethylation by free-living bacteria. In a more recent paper, Jackson and Muir [55] updated their interpretation and suggested that bacterial demethylation is responsible for the MIF in fish. However, recent studies demonstrated that microbial processes (microbial reduction, micro methylation and micro demethylation) are unlikely to cause Hg MIF [20–23]. Studies on human hair showed no *in vivo* MIF for people consuming fish [62,125]. Kwon et al. [68,69] performed

feeding experiments, and also demonstrated that Hg MIF signatures appears to be consistently unaffected by biochemical reactions within organisms.

Photo-induced reductions are the most common interpretation to the significant MIF in biological samples. It has been proposed that MIF signatures in aquatic food webs are originally generated in the water column by photo-reactions and subsequently transferred to the organism *via* food uptake and bioaccumulation [24]. The degree of MIF may be related to the Hg sources. Gantner et al. [122] studied the food web in arctic lakes, and found that pelagic zooplankton accumulating Hg directly from surface water showed significant MIF (Δ^{199}Hg: up to +3.4‰), while benthic chironomids that assimilate Hg from sediments had lower MIF (Δ^{199}Hg: +1.31‰). Senn et al. [48] compared the MIF signatures in oceanic and coastal fish. Oceanic fish have notably higher Δ^{201}Hg (+1.5‰) than those of coastal fish (+0.4‰), indicating oceanic MeHg having undergone substantial photo-degradation before entering the food web. Hg MIF in bio-monitors may provide key information on photochemical transformations of Hg [24]. Gantner et al. [122] observed a decreasing pattern between fish δ^{202}Hg and latitude in several Arctic Lakes. Hg MIF in marine seabird eggs from the Alaskan arctic revealed a pronounced latitudinal gradient in Δ^{199}Hg reflecting the influence of sea ice on surface ocean photo-degradation [126]. Day et al. [127] demonstrated latitude effect of Hg isotope signatures in seabird eggs.

6. Future directions

The field of Hg isotope geochemistry is rapidly emerging to be an important research area because analytical methods are now well established to measure Hg isotopes in many matrices. Isotope geochemistry of Hg has provided clearly defined tracers of sources, quantitative information on mixing, and identification of specific geochemical processes. A combination of well-established laboratory experiments and field data observations will be explored, which further widen the scope of Hg geochemistry, including global modeling, exploration geochemistry, and applied ecology. Considering the current progress, the following areas may need special attention in the future.

- **Improving sensitivity of Hg isotope measurements.** Advances in instrumentation and analytical techniques will continue to improve the precision and sensitivity of Hg isotope analysis, and it will be possible to identify and interpret more subtle isotope variations. Methods for high resolution (such as *in situ* analysis) need to be improved so that time-dependent variations could be resolved in sequentially-deposited layers and biological growth bands, *e.g.*, tree rings.
- **Measuring natural compound-specific Hg.** Hg is a prime example for the need of species-specific information in geochemistry studies. The different Hg species exhibit vastly different chemical, physical, and toxicological characteristics. It is therefore expected that isotope ratio measurements will follow previous analytical and environmental studies and use species-specific measurements to shed more light on the complex Hg biogeochemical cycle.
- **Establishing Hg isotope signature of major Hg reservoirs.** We are at the beginning stage of establishing the framework for the Hg isotope systems. It has shown evidences in Hg isotopic variations in different environmental compartments, which greatly upgrade our understanding on mercury sources. However, most of what we know today about natural Hg isotope variations is still very limited. Additional work is needed to extend it to all environmental compartments with low Hg concentrations (*e.g.*, precipitation, natural water and the atmosphere).
- **Defining Hg isotope fractionation during diagnostic geochemical processes.** With the increasing data reporting natural Hg isotopic variations, a critical issue for geochemists is to know how they are related to the global biogeochemical cycling of Hg. Unfortunately, our database of well-constrained Hg isotope fractionation factors is still very limited and requires rapid expansion to fully understand Hg isotope variations in nature. For instance, significant knowledge gaps still remain on mercury isotope fractionation during the entire atmospheric Hg cycle. As ocean plays a critical role in the global cycling of Hg, another hotspot on mercury isotope research may be associated to mercury cycling in oceans, *e.g.*, methylation/demethylation, bioaccumulation processes.

Acknowledgments

This research was funded by National "973" Program (2013CB430000), Natural Science Foundation of China (41303014, 41021062, and 41120134005), and a seed collaborative project from the State Key Laboratory of Marine Pollution.

References

[1] O. Lindqvist, K. Johansson, M. Aastrup, et al. Water Air Soil Pollut. 55 (1991) 193–216.
[2] W. Fitzgerald, D. Engstrom, R. Mason, et al. Environ. Sci. Technol. 32 (1998) 1.
[3] N. Selin, Annu. Rev. Environ. Resour. 34 (2009) 43–63.
[4] W. Schroeder, J. Munthe, Atmos. Environ. 32 (1998) 809–822.
[5] N. Pirrone, S. Cinnirella, X. Feng, et al. Atmos. Chem. Phys. 10 (2010) 5951–5964.
[6] X. Fu, X. Feng, Z. Dong, et al. Atmos. Chem. Phys. Discuss. 9 (2010) 23465–23504.
[7] H. Zhang, R. Yin, X. Feng, et al. Sci. Rep. 3 (2013) 3322.
[8] T. Douglas, S. Sturm, W. Simpson, et al. Environ. Sci. Technol. 42 (2008) 1542–1551.
[9] C. Lin, S. Pehkonen, Atmos. Environ. 33 (1999) 2067–2079.
[10] I. Hedgecock, N. Pirrone, Environ. Sci. Technol. 38 (2004) 69–76.
[11] J. Schaefer, J. Latowski, T. Barkay, Geomicrobiol. J. 19 (2002) 87–102.
[12] K. Gårdfeldt, M. Jonsson, J. Phys. Chem. A 109 (2003) 4478–4482.
[13] Z. Xiao, D. Strömberg, O. Lindqvist, Water Air Soil Pollut. 80 (1995) 789–798.
[14] M. Andersson, J. Sommar, K. Gårdfeldt, O. Marine, Chemistry 110 (2008) 190–194.
[15] B. Bergquist, J. Blum, Elements 5 (2009) 353–357.
[16] R. Yin, X. Feng, W. Shi, Appl. Geochem. 25 (2010) 1467–1477.
[17] J. Blum, Handbook of Environmental Isotope Geochemistry, Springer, Berlin, Germany, 2011, pp. 229–245.
[18] J. Sonke, Geochim. Cosmochim. Acta 75 (2011) 4577–4590.
[19] H. Hintelmann, Use of Stable Isotopes for Mercury Research. Mercury in the Environment: Pattern and Processes, University of California Press, California, 2012.
[20] K. Kritee, J. Blum, M. Johnson, et al. Environ. Sci. Technol. 41 (2007) 1889–1895.
[21] K. Kritee, J. Blum, T. Barkay, Environ. Sci. Technol. 42 (2008) 9171–9177.
[22] P. Rodríguez-González, V. Epov, C. Pecheyran, et al. Environ. Sci. Technol. 43 (2009) 9183–9188.
[23] K. Kritee, T. Barkay, J. Blum, Geochim. Cosmochim. Acta 73 (2009) 1285–1296.
[24] B. Bergquist, J. Blum, Science 318 (2007) 19.
[25] W. Zheng, H. Hintelmann, Geochim. Cosmochim. Acta 73 (2009) 6704–6715.
[26] W. Zheng, D. Foucher, H. Hintelmann, J. Phys. Chem. A. 114 (2010) 4246–4253.
[27] L. Yang, R. Sturgeon, Anal. Bioanal. Chem. 393 (2009) 377–385.
[28] W. Zheng, D. Foucher, H. Hintelmann, J. Phys. Chem. A 114 (2010) 4238–4245.
[29] M. Jiménez-Moreno, V. Perrot, V. Epov, et al. Chem. Geol. 336 (2013) 26–36.
[30] D. Malinovsky, K. Latruwe, L. Moens, et al. J. Anal. At. Spectrom. 25 (2010) 950–956.
[31] W. Zheng, D. Foucher, H. Hintelmann, J. Anal. At. Spectrom. 22 (2007) 1097–1104.
[32] N. Estrade, J. Carignan, J. Sonke, et al. Geochim. Cosmochim. Acta 73 (2009) 2693–2711.
[33] J. Wiederhold, K. Daniel, I. Infante, et al. Environ. Sci. Technol. 44 (2010) 4191–4197.
[34] M. Jiska, J. Wiederhold, B. Bourdon, et al. Environ. Sci. Technol. 6 (2012) 6654–6662.
[35] R. Yin, X. Feng, J. Wang, et al. Chem. Geol. 336 (2013) 80–86.
[36] P.G. Koster van Groos, B. Esser, R. Williams, et al. Environ. Sci. Technol. 48 (1) (2014) 227–233.
[37] D. Foucher, H. Hintelmann, Anal. Bioanal. Chem. 384 (2006) 1470–1478.
[38] A. Biswas, J. Blum, B. Bergquist, et al. Environ. Sci. Technol. 42 (2008) 8303–8309.
[39] D. Foucher, N. Ogring, H. Hintelmann, Environ. Sci. Technol. 43 (2009) 33–39.
[40] D. Foucher, H. Hintelmann, T. Al, et al. Chem. Geol. 336 (16) (2013) 87–95.
[41] G. Gehrke, J. Blum, P. Meyers, Geochim. Cosmochim. Acta 73 (2009) 1651–1665.
[42] G. Gehrke, J. Blum, M. Marvin-DiPasquale, Geochim. Cosmochim. Acta 75 (3) (2011) 691–705.
[43] N. Estrade, J. Carignan, O. Donard, Environ. Sci. Technol. 44 (16) (2010) 6062–6067.

[44] N. Estrade, J. Carignan, O. Donard, Environ. Sci. Technol. 45 (4) (2011) 1235–1242.
[45] X. Feng, D. Foucher, H. Hintelmann, et al. Environ. Sci. Technol. 44 (2010) 3363–3368.
[46] X. Feng, R. Yin, B. Yu, et al. Chin. Sci. Bull. 58 (2) (2013) 249–255.
[47] J. Sonke, J. Schaefer, J. Chmeleff, et al. Chem. Geol. 279 (2010) 90–100.
[48] D. Senn, E. Chesney, J. Blum, et al. Environ. Sci. Technol. 44 (2010) 1630–1637.
[49] W. Shi, X. Feng, G.L. Zhang, et al. Chin. Sci. Bull. 56 (9) (2011) 877–882.
[50] L. Sherman, J. Blum, G. Keeler, et al. Environ. Sci. Technol. 46 (1) (2012) 382–390.
[51] J. Liu, X. Feng, R. Yin, et al. Chem. Geo. (2011), http://dx.doi.org/10.1016/j.chemgeo.2011.06.001.
[52] R. Yin, X. Feng, J. Wang, et al. Chem. Geol. 336 (2013) 87–95.
[53] P.M. Donovan, J.D. Blum, D. Yee, et al. Chem. Geol. 349–350 (2013) 87–98.
[54] T. Jackson, D. Muir, W. Vincent, Environ. Sci. Technol. 38 (2004) 2813–2821.
[55] T. Jackson, D. Muir, Sci. Total Environ. 417–418 (2012) 189–203.
[56] T. Jackson, K. Telmer, D. Muir, Chem. Geol. 352 (2013) 27–46.
[57] T. Jackson, Chem. Geol. 355 (2013) 88–102.
[58] C. Smith, S. Kesler, B. Klaue, et al. Geology 33 (2005) 825–828.
[59] T. Jackson, D. Whittle, M. Evans, et al. Geochim. Cosmochim. Acta 70 (18S) (2006) A284.
[60] T. Jackson, D. Whittle, M. Evans, et al. Appl. Geochem. 23 (2008) 547–571.
[61] J. Carignan, N. Estrade, J. Sonke, et al. Environ. Sci. Technol. 243 (2009) 5660–5664.
[62] L. Laffont, J. Sonke, L. Maurice, et al. Environ. Sci. Technol. 45 (23) (2011) 9910–9916.
[63] L. Sherman, J. Blum, D. Nordstrom, et al. Earth Planet. Sci. Lett. 29 (2009) 86–96.
[64] L. Sherman, J. Blum, K. Johnson, et al. Nat. Genet. 3 (2010) 173–177.
[65] L. Sherman, J. Blum, T. Douglas, et al. J. Geophys. Res. 117 (D14) (2011).
[66] G. Gehrke, J. Blum, D. Slotton, et al. Environ. Sci. Technol. 45 (4) (2013) 1264–1270.
[67] V. Perrot, V. Epov, M. Pastukhov, et al. Environ. Sci. Technol. 44 (21) (2010) 8030–8037.
[68] S. Kwon, J. Blum, M. Carvan, et al. Environ. Sci. Technol. 46 (2012) 7527–7534.
[69] S. Kwon, J. Blum, M. Chirby, et al. Environ. Toxicol. Chem. 32 (10) (2013) 2322–2330.
[70] S. Ghosh, Y. Xu, M. Humayun, et al. Geochem. Geophys. Geosyst. 9 (2008).
[71] R. Yin, X. Feng, B. Meng, Environ. Sci. Technol. 47 (5) (2013) 2238–2245.
[72] J. Blum, B. Popp, J. Drazen, et al. Nat. Geosci. 6 (2013) 879–884.
[73] B. Klaue, S. Kesler, J. Blum, Presented at the Annual International Conference on Heavy Metals in the Environment, Ann Arbor, MI, USA, Contribution 1201, 2000.
[74] J. Sonke, J. Blum, Chem. Geol. 336 (2013) 1–4.
[75] J. Blum, B. Bergquist, Anal. Bioanal. Chem. 388 (2007) 353–359.
[76] E. Young, A. Galy, H. Nagahara, Geochim. Cosmochim. Acta 66 (6) (2002) 1095–1104.
[77] H. Hintelmann, W. Zheng, Environ. Chem. Toxicol. Mercury (2011) 293–327.
[78] F. Aston, Nature 105 (1920) 617.
[79] J. Brønsted, G. von Hevesy, Nature 106 (1920) 144.
[80] A. Nier, Phys. Rev. 79 (1950) 450–454.
[81] N. Koval, V. Zakharchenko, O. Savin, et al. Dokl. Akad. Nauk SSSR 235 (1977) 936–938.
[82] D. Lauretta, B. Klaue, J. Blum, et al. Geochim. Cosmochim. Acta 65 (2001) 2807–2818.
[83] R. Evans, H. Hintelmann, P. Dillon, J. Anal. At. Spectrom. 16 (2001) 1064–1069.
[84] T. Jackson, Can. J. Fish. Aquat. Sci. 58 (2001) 185–196.
[85] B. Klaue, J. Blum, U.K. Goldschmidt Conference Oxford, J Conf. Abs 5 (2) (2000) 591.
[86] F. Stellaard, H. Elzinga, Isotopes Environ. Health Stud. 41 (4) (2005) 345–361.
[87] H. Hintelmann, S.Y. Lu, Analyst 128 (2003) 635–639.
[88] J. Sonke, T. Zambardi, T. Toutain, J. Anal. Atom. Spectrom. 23 (2008) 569–573.
[89] R. Yin, X. Feng, D. Foucher, et al. Chin. J. Anal. Chem. 38 (2010) 929–934.
[90] C. Mead, J. Lyons, T. Johnson, et al. Environ. Sci. Technol. 47 (2013) 2542–2547.
[91] N. Estrade, J. Carignan, J. Sonke, et al. Geostand. Geoanal. Res. 34 (2010) 79–93.
[92] R. Evans, H. Hintelmann, P. Dillon, J. Anal. Atom. Spectrom. 9 (2001) 1064–1069.
[93] Q. Xie, S. Lu, D. Evans, et al. J. Anal. Atom. Spectrom. 20 (2005) 515–522.
[94] M. Dzurko, D. Foucher, H. Hintelmann, Anal. Bioanal. Chem. 393 (2009) 345–355.
[95] V. Epov, P. Rodriguez-Gonzalez, J. Sonke, et al. Anal. Chem. 80 (2008) 3530–3538.
[96] V. Perrot, M. Jimenez-Moreno, S. Berail, et al. Chem. Geol. 355 (26) (2013) 153–162.
[97] R. Sun, M. Enrico, L.E. Heimbürger, et al. Anal. Bioanal. Chem. 405 (21) (2013) 6771–6781.
[98] J. Chen, H. Hintelmann, B. Dimock, J. Anal. At. Spectrom. 25 (2010) 1402–1409.
[99] L. Gratz, G. Keeler, J. Blum, et al. Environ. Sci. Technol. 44 (2010) 7764–7770.
[100] T. Zambardi, J. Sonke, J. Toutain, et al. Earth Planet. Sci. Lett. 277 (2009) 236–243.
[101] J. Rolison, W. Landing, W. Luke, et al. Chem. Geol. 336 (2013) 37–49.
[102] Hoefs, Stable Isotope Geochemistry, Springer-Verlag, Berlin, Germany, 2009.
[103] Y. Amelin, D. Davis, W. Davis, Geochim. Cosmochim. Acta 69 (2005) A215.
[104] V. Epov, D. Malinovskiy, F. Vanhaecke, et al. J. Anal. At. Spectrom. 26 (2011) 1142–1156.
[105] E. Schauble, Geochim. Cosmochim. Acta 71 (2007) 2170–2189.
[106] S. Ghosh, E. Schauble, G. Couloume, et al. Chem. Geol. 336 (2013) 5–12.
[107] A. Buchachenko, V. Ivanov, V. Roznyatovskii, et al. Doklady Phys. Chem. 413 (2007) 39–41.
[108] C. Grissom, Chem. Rev. 95 (1995) 3–24.
[109] A. Buchachenko, D. Kouznetsov, A. Shishkov, J. Phys. Chem. 108 (2004) 707–710.
[110] J. Chen, H. Hintelmann, X. Feng, et al. Geochim. Cosmochim. Acta 90 (2012) 33–46.
[111] J. Demers, J. Blum, D. Zak, Global Biogeochem. Cycles 27 (2013) 222–238.
[112] C.T. Driscoll, R.P. Mason, H.M. Chan, D.J. Jacob, N. Pirrone, Environ. Sci. Technol. 47 (10) (2013) 4967–4983.
[113] C. Smith, S. Kesler, J. Blum, et al. Earth Planet. Sci. Lett. 269 (2008) 399–407.
[114] R. Yin, X. Feng, Q. Zhang, et al. Appl. Geochem. 27 (1) (2012) 151–160.
[115] J. Wiederhold, R. Smith, H. Siebner, et al. Environ. Sci. Technol. 47 (2013) 6137–6145.
[116] S. Stetson, J. Gray, R. Wanty, et al. Environ. Sci. Technol. 43 (2009) 7331–7336.
[117] J. Gray, M. Pribil, P. Higueras, Chem. Geol. 357 (2013) 150–157.
[118] L. Lefticariu, J. Blum, J. Gleason, Environ. Sci. Technol. 45 (2011) 1724–1729.
[119] R. Sun, L.-E. Heimbürger, J. Sonke, et al. Chem. Geol. 336 (2013) 103–111.
[120] L.S. Sherman, J.D. Blum, G. Keeler, et al. Environ. Sci. Technol. 46 (1) (2012) 382–390.
[121] J. Gray, M. Pribil, P. Metre, et al. Appl. Geochem. 29 (2013) 1–12.
[122] N. Gantner, H. Hintelmann, W. Zheng, et al. Environ. Sci. Technol. 43 (2009) 9148–9154.
[123] R. Das, V. Salters, A. Odom, Geochem. Geophys. Geosyst. 10 (2012) Q11012.
[124] V. Perrot, M. Pastukhov, V. Epov, et al. Environ. Sci. Technol. 46 (2012) 5902–5911.
[125] L. Laffont, J. Sonke, L. Maurice, et al. Environ. Sci. Technol. 43 (2009) 8985–8990.
[126] D. Point, J. Sonke, R. Day, et al. Nat. Geosci. 4 (2011) 188–194.
[127] R. Day, D. Roseneau, S. Berail, et al. Environ. Sci. Technol. 46 (2012) 5327–5335.